minerals

MDPI

Article

The Delineation of Copper Geochemical Blocks and the Identification of Ore-Related Anomalies Using Singularity Analysis of Stream Sediment Geochemical Data in the Middle and Lower Reaches of the Yangtze River and Its Adjacent Areas, China

Bin Liu [1,2], Xingtao Cui [1,*] and Xueqiu Wang [3,4]

[1] Institute of Resource and Environmental Engineering, Hebei GEO University, Shijiazhuang 050031, China; 13488156587@163.com
[2] Hebei Key Laboratory of Strategic Critical Mineral Resources, Hebei GEO University, Shijiazhuang 050031, China
[3] Key Laboratory of Geochemical Exploration, Institute of Geophysical and Geochemical Exploration, Langfang 065000, China; wangxueqiu@igge.cn
[4] UNESCO International Centre on Global-Scale Geochemistry, Langfang 065000, China
* Correspondence: cxt78520@126.com

Abstract: The middle and lower reaches of the Yangtze River and its adjacent areas contain abundant mineral resources, especially porphyry–skarn–stratabound Cu–Au–Mo–Fe deposits, and still have great potential for mineral prospecting. In this paper, geochemical blocks and local singularity mapping methods were used to delineate the spatial distribution pattern of Cu and identify the geochemical anomalies related to Cu deposits. Six copper geochemical blocks, each with an area of more than 1000 km^2, were all spatially consistent with the locations of the five Cu ore districts (Edongnan, Jiurui, Anqing-Guichi, Tongling, and Ningzhen) and one ore field (Dexing) in the study area. Thus, geochemical blocks delineated with low-density geochemical data can effectively track the locations of ore districts or large ore deposits. Most of the known Cu deposits in the study area were located in anomalous areas with singularity indices less than 1.741 in the Cu singularity map. The singularity analysis could reduce the anomalous areas and identify the geochemical anomalies related to Cu deposits effectively. Geochemical blocks combining a local singularity mapping method is an effective tool for identifying prospecting targets.

Keywords: the middle and lower reaches of the Yangtze River; geochemical block; singularity analysis; ore-related anomalies

check for updates

Citation: Liu, B.; Cui, X.; Wang, X. The Delineation of Copper Geochemical Blocks and the Identification of Ore-Related Anomalies Using Singularity Analysis of Stream Sediment Geochemical Data in the Middle and Lower Reaches of the Yangtze River and Its Adjacent Areas, China. *Minerals* **2023**, *13*, 1397. https://doi.org/10.3390/min13111397

Academic Editor: Paul Alexandre

Received: 15 August 2023
Revised: 25 October 2023
Accepted: 28 October 2023
Published: 31 October 2023

Copyright: © 2023 by the authors. Licensee MDPI, Basel, Switzerland. This article is an open access article distributed under the terms and conditions of the Creative Commons Attribution (CC BY) license (https://creativecommons.org/licenses/by/4.0/).

1. Introduction

One of the fundamental problems of exploration geochemistry is how to enhance anomalies by extracting anomalies in the selection and analysis of sampling media and how to identify and interpret anomalies by processing geochemical data with different mathematical models and technologies [1–6]. Determining the content and spatial distribution of geochemical elements are the prerequisites for effectively delineating geochemical anomalies. The spatial distribution pattern of geochemical elements is constrained by a number of factors, such as rocks with high background values, the enrichment of elements caused by mineralization, and the secondary dispersion of elements after mineralization weathering [7]. By studying the relationship between geochemical blocks and ore districts or large/giant deposits, Wang et al. (2007) pointed out that ore districts or large ore deposits are generally produced in geochemical blocks [8]. Therefore, how to effectively identify mineralization-related anomalies is the key to mineral prediction and exploration.

There is a hierarchy of nested geochemical patterns in stream sediment, such as local anomalies (<100 km^2), regional anomalies (100~1000 km^2), geochemical province (1000~10,000 km^2), giant geochemical province (10,000~100,000 km^2), and geochemical domain (100,000~1,000,000 km^2). They are actually the display of huge rock blocks rich in one or several metal elements on the earth's surface [9]. A geochemical province can be defined as a relatively large area of the earth's crust in which the concentration of a certain geochemical element or elements is significantly higher than the average value of the whole crust, and it can provide important exploration clues. We name geochemical anomalies with a certain thickness larger than 1000 km^2 geochemical blocks [9,10]. There is a close relationship between geochemical blocks and ore districts [2,8,11]. These geochemical blocks, which are rich in one or several metal elements, can provide the necessary material for the formation of deposits. The introduction of geochemical blocks is of great significance for the effective discovery of new ore districts or large/giant deposits [8].

Due to the long-term, complex, and superposition of the geological mineralization process, the data sets that record the process often have characteristics of non-stationary and non-linear structures [4,12,13]. Zhao et al. (1994) have pointed out that the main causes limiting mineral prediction accuracies and effective mineral exploration are the inadequate acquisition of mineralization information and the limitations of linear prediction models [14]. Methods of fractal and multifractal analyses have already been adopted in identifying anomalies from background data [15,16]. Specifically, they include the concentration–area model (C–A) [17–19], number–size model (N–S) [20–22], concentration–volume model (C–V) [23], concentration–distance model (C–D) [24], spectrum–area model (S–A) [25], and local singularity model [26]. The local singularity index introduced by Cheng (2007) can provide new information that could help to complement the use of original concentration values and quantify the enrichment and depletion caused by mineralization. The local singularity index is widely recognized as a useful tool to distinguish relatively weak anomalies in complex geological backgrounds and the singularity mapping technique can detect local and mineralization-related weak anomalies [26–32].

The middle-lower Yangtze River region is one of the most important polymetallic metallogenic belts in China, hosting plenty of porphyry–skarn–stratabound Cu–Au–Mo–Fe deposits [33]. More than 200 deposits of various kinds have been found. People used to focus on geology and geochemical characteristics, ore-controlling structures, metallogenic dynamics, geochronology, and isotopes to conduct mineral exploration in this region [34–38]. Large areas of Cu anomalies in this region have been delineated through geochemical block theory [39–42], which show the great potential of this area for prospecting In this paper, the middle and lower reaches of the Yangtze River and its adjacent areas (28°~32°40′ N; 114°~120° E) were selected as the study area. Two approaches, the geochemical block theory and the local singularity mapping method were adopted to achieve the following objectives: (1) to determine the relationship between geochemical anomalies and geological background and between geochemical anomalies and mineralization and (2) to identify geochemical anomalies caused by Cu mineralization.

2. Geological Setting

The middle-lower Yangtze River polymetallic metallogenic belt is located in the convergence zone of the North China plate and the Yangtze plate. It is bound to the north by the Xiangfan Guangji and the Tanlu faults and to the south by the Yangxing Changzhou faults. The region is controlled by the Tethys tectonic domain, the ancient Pacific tectonic domain, and the deep crust–mantle process together [34,35,37].

The strata of the study area are distributed from Precambrian to Quaternary. Among them, Archean–Proterozoic and Neoproterozoic metamorphic basements are sporadically displayed in the study area, while the Cambrian–Early Triassic clastic rocks and carbonate rocks and the Jurassic–Cretaceous continental volcanic rocks mingled with clastic rocks are widely distributed in the study area. The deposits are mainly found in the Carboniferous–Triassic strata (Figure 1) [43,44].

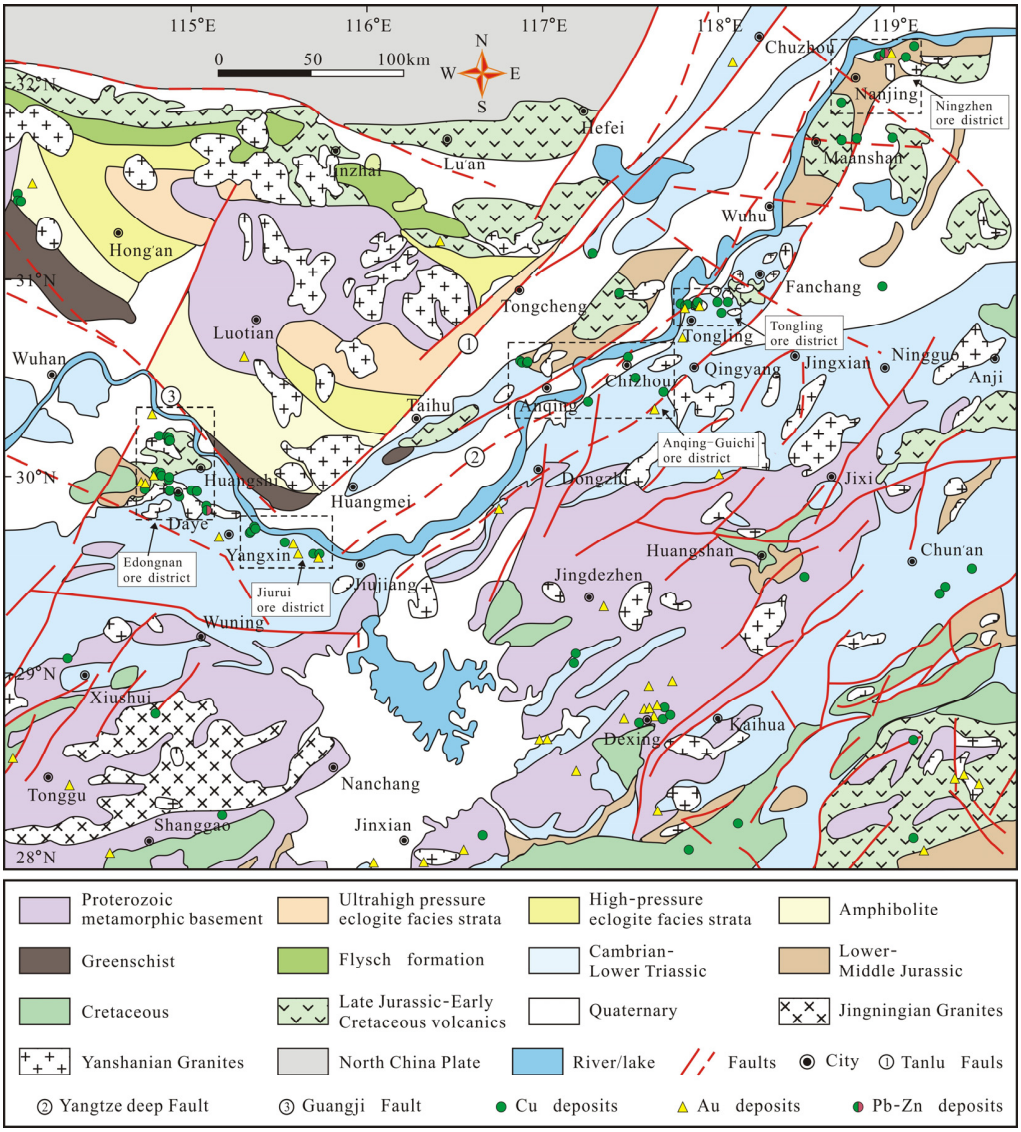

Figure 1. Simplified geological map of the middle and lower reaches of the Yangtze River and its adjacent areas [45].

In terms of tectonics, NNE trending faults mostly developed in the middle-lower Yangtze River region. Magmatic activities and deposit distributions are obviously controlled by them. At the same time, in this region, there are also E-W and NE-SW trending faults. The intersection of faults with different directions is most favorable for mineralization [34,35].

Magmatic rocks are widely distributed in the study area and are mainly composed of three series: high potassic calC–Alkaline series, mugearite series, and alkaline granite series [34,37,46,47]. The formation of intermediate-acid magmatic rocks, which are most closely related to metallogenesis, is related to crust–mantle interaction. The underplating of Mesozoic basal magma and the interaction between crust and mantle have led to the formation of granitic rocks [37,48,49]. The mugearite is mainly distributed along the Yangtze River in several volcanic basins, such as the Huaining basin, the Luzong basin, and the Ningwu basin [46,50].

The mineralizations of the middle-lower Yangtze River region were mainly formed in 145~130 Ma [38]. The types of deposits are diverse and complicated. The types of mineralization can be divided into the skarn–porphyry Cu mineralization caused by high potassic calC–Alkaline granite; the "porphyrite iron ore" mineralization caused by mugearite in the

volcanic basins; the oxides–Cu–Au mineralization caused by A-type granite; and Au, Sb, Pb, and Zn mineralization which is not obviously related to magmatic activities [49]. At present, five Cu ore districts have been found, namely, the Edongnan, Jiurui, Anqing-Guichi, Tongling, and Ningzhen ore districts.

3. Data and Methods

3.1. Stream Sediment and Rock Geochemical Data

In this paper, 62,344 stream sediment samples covering the middle and lower reaches of the Yangtze River and its adjacent areas were selected, which were derived from the Regional Geochemistry-National Reconnaissance Project (RGNR) [8,51]. The sampling density was 1 sample/km^2, and 4 adjacent samples were combined into one analytical sample. A total of 39 elements were tested. More details of sampling and analysis methods of stream sediment geochemical data can be found in Xie et al. (1997) [51].

To interpret the geogenic sources of Cu elements, we used an additional 622 rock samples in the study area (Figure 2) from the China Geochemical Baselines (CGB). The CGB was launched in 2008 and completed in 2012. The rock samples in the CGB were collected in areas with no mineralized alteration. Concentrations of Cu in the rock samples were analyzed by inductively coupled plasma mass spectrometry. More details of the sampling and chemical analysis are available in Wang and the CGB Sampling Team (2015) [6].

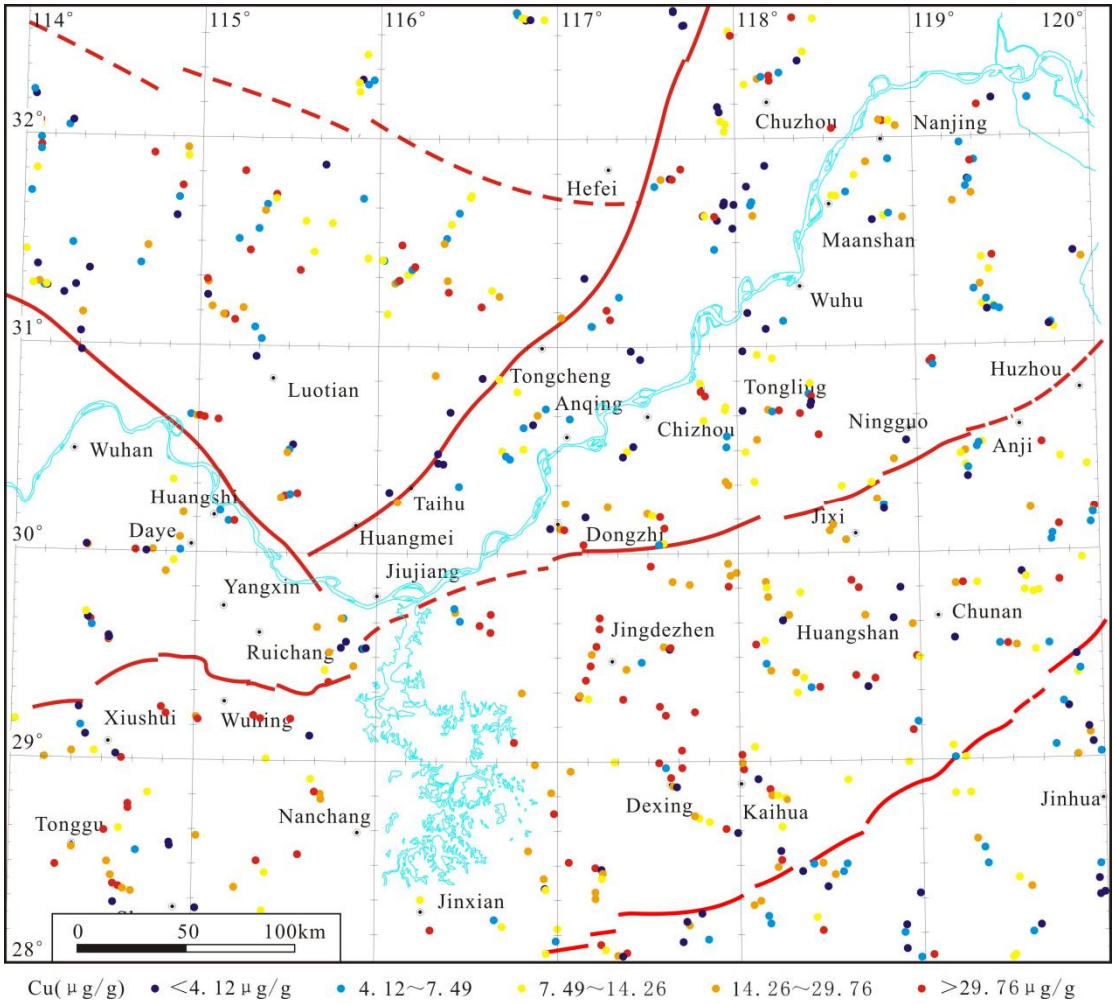

Figure 2. Locations of 622 rock samples marked by colored dots in the middle and lower reaches of the Yangtze River and its adjacent areas. The five colored dot classes are based on the following percentiles of raw data: <20% (dark blue), ≥20 to <40% (blue), ≥40 to <60% (yellow), ≥60 to ≤80% (orange), and >80% (red) Cu content.

3.2. Geochemical Block of Cu

Doe (1991) first presented the term geochemical block to identify a very large rock mass that has a high content of a certain element or elements [52]. However, there were no reliable data to support this concept. Xie (1995) proposed using regional geochemical prospecting data to delineate geochemical blocks [10]. Geochemical patterns with a certain thickness (e.g., 500 m), which have an area of >1000 km^2 and more than three layers of nested structures, are recognized as geochemical blocks [9,10,53].

Since the density of one sample per 4 km^2 is too high, the geochemical data of the original sediments were averaged before the geochemical anomaly delineation. By obtaining one average value from each 10 km × 10 km grid square (approximately one average value per 100 km^2), we can obtain 2621 new low-density composite data.

The compilation of the spatial distribution of copper geochemical blocks in the study area was conducted through the GeoChem Studio 1.5 software developed by the Institute of Geophysical and Geochemical Exploration [54–56]. In the GeoChem Studio 1.5 system data processing module, the discrete data were meshed by inversely proportioning the distance power function; the search radius was 25 km. On the basis of the grid, different gradations were used to represent different levels of blocks. The cumulative frequency of 85% was used as the threshold of copper geochemical blocks, and the cumulative frequencies of 92% and 98% were used for color gradation.

3.3. Local Singularity Mapping Method

The singularity proposed by Cheng (2007) was described as a phenomenon in geology where a great deal of energy can be released or a large amount of material can be accumulated in a very small time-space limit. Geological anomalies caused by non-linear geological processes are consistent with the singularity theory [26], such as hydrothermal mineralization. The phenomenon is normally characterized by self-similarity or scale-invariant properties based on the multifractal theory. Therefore, the singularity model can be defined as a power–law relationship as follows [26]:

$$X[A(\varepsilon)] = c\ \varepsilon^{\alpha-2} \quad (1)$$

where $A(\varepsilon)$ is a given area, $X[A(\varepsilon)]$ is the average concentration, ε is a normalized distance measure such as window size, c is a constant value, and α is the singularity index [57].

In a 2-dimension geochemical map, when the singularity index a is close to 2, the area is normal and has not been affected too much by mineralization. When the singularity index a is smaller than 2, the area is element-enriched by mineralization or other local geological processes. When the singularity index a is greater than 2, the area is element-depleted by mineralization [26]. Therefore, the singularities deduced from a geochemical map can be used to identify patterns with singular element concentration values, which can offer valuable information to interpret geochemical anomalies caused by mineralization.

The local singularity index α can be obtained through the window-based method based on either raw point geochemical data or raster maps [26,29]. Firstly, locate sampling points on a map and then define a set of sliding windows $A(r_i)$ with variable window sizes ($r_{min} = r_1 < r_2 < r_3 \ldots < r_n = r_{max}$). Secondly, calculate the average concentration $X[A(r_i)]$ ($i = 1, \ldots, n$) in each window area. Finally, plot the window size r_i and values of $X[A(r_i)]$ on log–log graph and then obtain the linear relationship $\mathrm{Log}\ X[A(r_i)] = c + (\alpha - 2)\ \mathrm{Log}(r_i)$. The value of $\alpha - 2$ can be obtained from the estimation of the slope of the straight line. Similar treatment with sliding windows at all locations on the geochemical map can produce a singularity distribution map [26,30].

To map the α-values of the stream sediment Cu concentrations in the middle and lower reaches of the Yangtze River and its adjacent areas, we calculated the average concentration of the original sediments for each 4 km × 4 km grid square (approximately one sample per 16 km^2) and obtained a total of 15,613 points. The average was placed at the center point of each grid square. The GeoDAS GIS 4.0 software [25] was used to map the distributions

of α-values in the study area. The optimum window size is usually determined based on experience. In this paper, the square windows with half window sizes were set to 2, 6, 10, 14, 18, and 22 km, with an interval of 4 km.

The optimal threshold of the α-value can be quantitatively determined using the Student statistic (*t*-value) provided by the weights of evidence method. Using this threshold, the α-value can be divided into two intervals, that is, the intervals that are favorable and unfavorable to the deposit distribution. In this study, we applied a *t*-value to quantitatively measure the spatial correlation between $\alpha < 2$ regions and known deposit locations. The larger the *t*-value is, the stronger the spatial correlation is. Generally, $t > 1.96$ can be considered as statistically significant [26]. The *t*-value can be calculated by the following formula:

$$t = C/S\,(C) \quad (2)$$

where $C = W^+ - W^-$ and S(C) is the standard deviation of C. W^+ and W^- are the weights when evidential patterns (e.g., geochemical anomalies) are present and absent, respectively.

4. Results

4.1. Statistical Characteristics of Cu

The skewness and kurtosis of the Cu concentrations after logarithmic transformation in the stream sediments were −2.14 and 8.28, respectively, indicating that the data had a negative skewness distribution (Figure 3a). Combined with the Q–Q plot (Figure 3b), we could observe that the data did not obey a normal distribution. The skewness and kurtosis of the Cu concentrations after logarithmic transformation in the rocks were 0.17 and −0.51, respectively, which indicated that the data had a positive skewness distribution (Figure 3c). Combined with the Q–Q plot (Figure 3d), we could observe that the data did not fully follow the normal distribution. The histogram of the Cu concentrations after logarithmic transformation in the rocks had a bimodal pattern, indicating that the middle and lower reaches of the Yangtze River and its adjacent areas have undergone various geological events or processes.

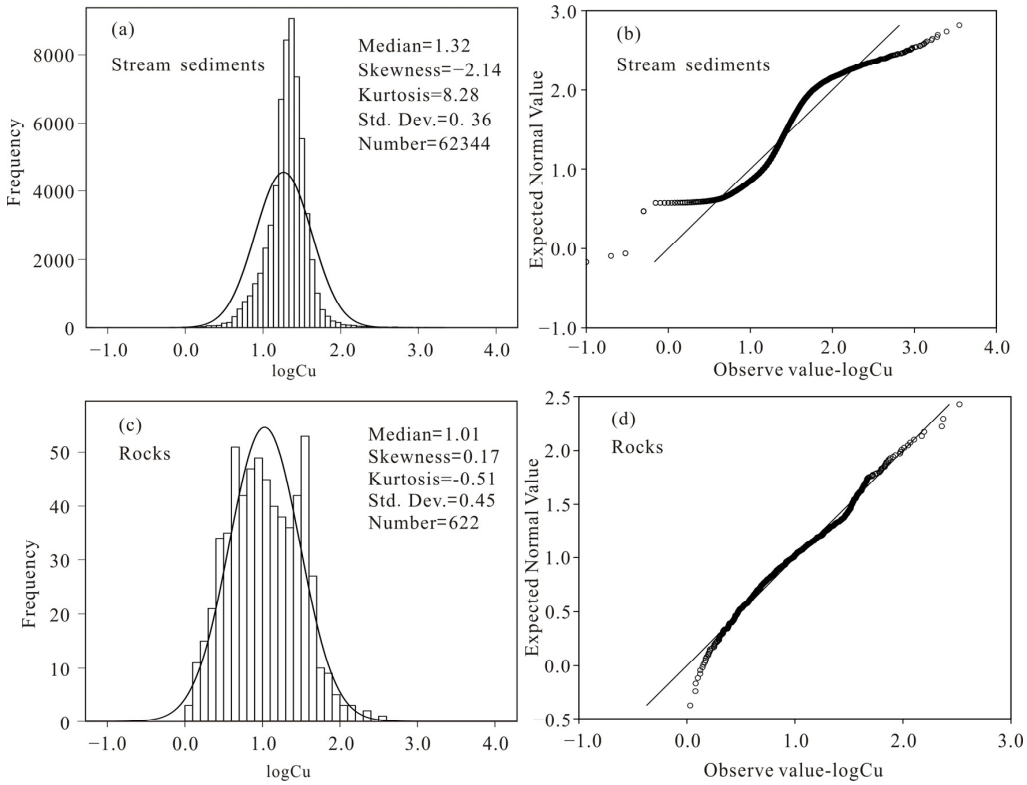

Figure 3. Histograms and Q–Q plots of Cu in the stream sediments (**a**,**b**) and rocks (**c**,**d**).

4.2. Copper Geochemical Blocks

Six copper geochemical blocks (Cu1, Cu2, Cu3, Cu4, Cu5, and Cu6) with Cu threshold values of more than 32 μg/g were delineated in the middle and lower reaches of the Yangtze River and its adjacent areas. The spatial distributions of copper geochemical blocks are shown in Figure 4.

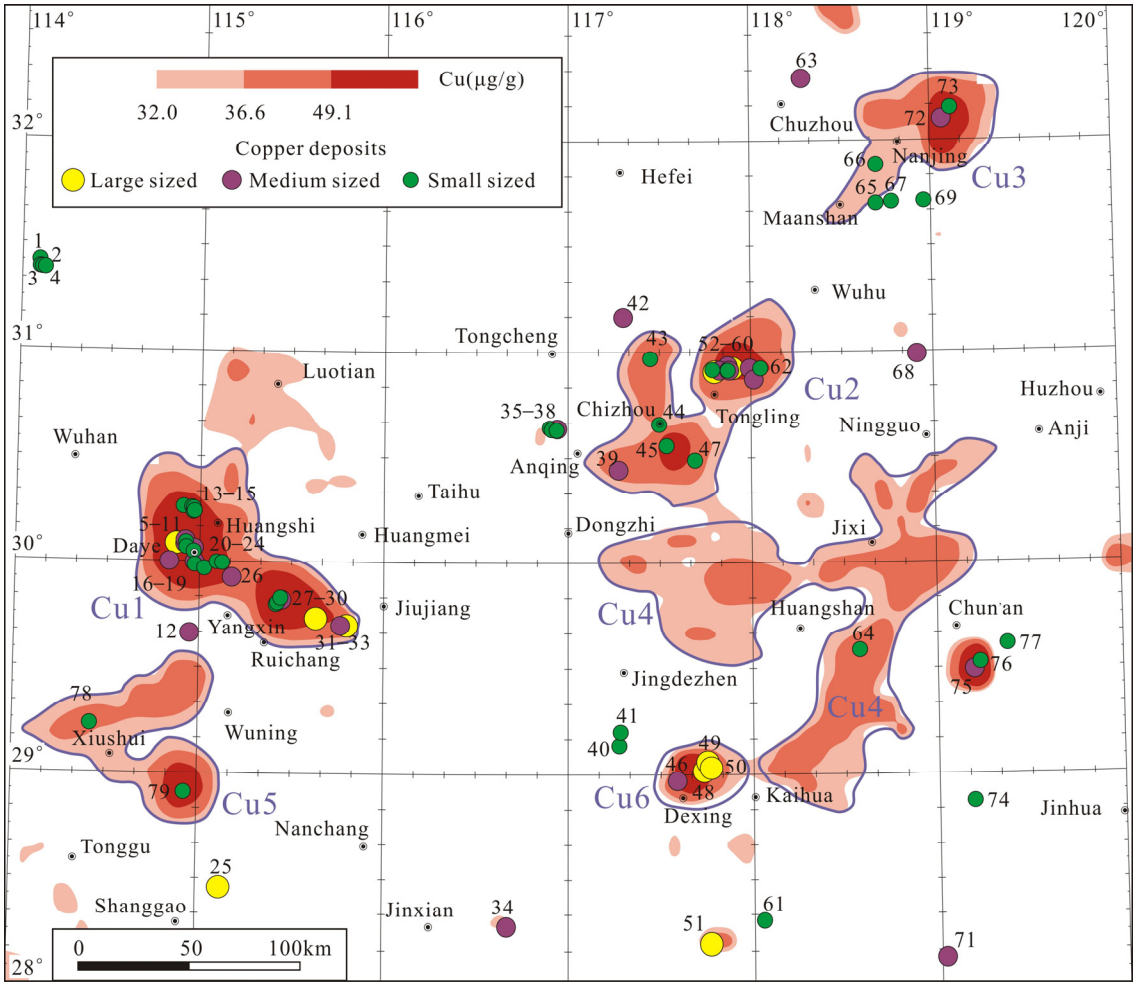

Figure 4. Spatial distributions of copper geochemical blocks in the middle and lower reaches of the Yangtze River and its adjacent areas.

The copper geochemical block Cu1 is located in the western part of the Daye-Jiujiang area and covers an area of 6760 km^2. The strata exposed in this area are mainly Upper Ordovician–Upper Jurassic, especially the Lower Triassic Daye group. The geochemical block Cu1 had a three-layered structure and two obvious anomaly-concentrated centers. The Edongnan and Jiurui ore districts are located in this geochemical block. Typical known deposits in this area include Tonglushan large-sized Cu–Co–Mo (No. 6), Tongshankou medium-sized Cu–Mo (No. 5), Jiguanzui medium-sized Cu–Co–Mo (No. 8), Taohuazui medium-sized Cu (No. 10), Shitouzui medium-sized Cu–Mo (No. 17), and Ruanjiawan medium-sized Cu–W–Mo (No. 26) deposits in the Edongnan ore district and Wushan large-sized Cu (No. 31), Chengmenshan large-sized Cu–Zn–Mo (No. 33), Fengsandong medium-sized Cu (No. 30), and Dingjiashan medium-sized Cu–Zn (No. 32) deposits in the Jiurui ore district. The geochemical block Cu1 also contains a series of small-sized Cu deposits (Nos. 7, 9, 11, 13–16, 18–20, 22–24, and 27–29).

The copper geochemical block Cu2 is located in the Anqing-Tongling area, with an area of 5978 km^2. The Devonian–Triassic strata is a favorable part of mineralization. The Yanshanian granite magma intrusion activities are strong and are characterized by large-scale

magmatic rock mass intrusions and continental volcanic eruptions. The mineralizations in this area are closely related to the volcanic eruptions and magmatic activities. The copper geochemical block Cu2 has a three-layer nested structure with two obvious anomaly-concentrated centers. The Anqing–Guichi and Tongling ore districts are located in the concentrated center of this copper geochemical block. Tongshan middle-sized Cu (No. 39), Tongguanshan large-sized Cu (No. 53), Dongguashan large-sized Cu (No. 58), Datuanshan middle-sized Cu (No. 55), Xinqiao middle-sized Cu–Au–S (No. 59), and Fenghuangshan middle-sized Cu–Co (No. 60) deposits are distributed in geochemical block Cu2. A number of small-sized Cu deposits (Nos. 43, 44, 45, 47, 52, 56, and 62) can also be found in this copper geochemical block.

The copper geochemical block Cu3 is located in the Ma'anshan-Nanjing area, in the northeast of the study area, and covers an area of 3611 km^2. In this area, the Sinian–Quaternary strata are exposed, containing carbonatite, fine clastic rocks, and a small amount of volcanic clastic rocks. This copper geochemical block has a three-layer nested structure. The Ningzhen ore district is distributed in this area. The Anjishan middle-sized Cu–Pb–Zn–Mo deposit (No. 72) and two small-sized Cu deposits (Nos. 66 and 73) are produced here.

The copper geochemical block Cu4 is located in the southeastern part of the study area, the Dongzhi–Jixi–Ningguo-Kaihua area, with an area of 13,602 km^2. The stratums of this geochemical block are mainly Neoproterozoic and Lower Paleozoic. The lithology is mainly marine carbonaceous siliceous rocks, dolomitic sandstone, carbonaceous siltstone, and carbonaceous limestone. The intrusions of early Yanshanian granites are exposed in this area, which are mainly composed of biotite granite–biotite adamellite–granitic diorite. This copper geochemical block has a two-layer nested structure, and no large Cu deposit has been found so far. The Panjia small-sized Cu–Zn (No. 64) deposit was discovered in the geochemical block Cu4.

The copper geochemical block Cu5 is distributed in the Xiushui–Wuning area in the southwestern part of the study area, with an area of 4990 km^2. The strata exposed here are mainly Mesoproterozoic and Sinian. In terms of magmatic activity, the Jinningian granodiorite, late Variscan granite, and early Yanshanian granite are widely distributed in this area. The geochemical block Cu5 has a three-layer nested structure with one obvious anomaly-concentrated center. Only two small-sized Cu deposits were discovered in this area.

The copper geochemical block Cu6 is located in the south part of the study area, the Dexing area, with an area of 1146 km^2. The Neoproterozoic, Paleozoic, and Mesozoic strata are exposed in this area, and the lithology is mainly palimpsest greywacke, slate, schist, and gneiss, and also contains basal volcanic lava. The intrusions of the Middle and Late Jurassic are widely exposed, and the lithology is mainly biotite monzogranite and granodiorite porphyry. The mineralization is closely related to Early Yanshanian granodiorite porphyry. This copper geochemical block has a three-layer nested structure with one obvious anomaly-concentrated center. The famous Dexing ore field, which consists of Tongchang large-sized Cu–Mo (No. 49), Fujiawu large-sized Cu–Mo (No. 50), Zhushahong large-sized Cu–Mo (No. 48), and Yinshan middle-sized Cu–Pb–Zn (No. 46) deposits, is located in this area.

4.3. Singularity Analysis

Singularity indices of Cu are normally distributed with an average value of 2.043 (Figure 5a). The spatial distribution of local singularity indices of Cu in the study area is shown in Figure 6. Areas with non-singular element concentration have singularity indices close to 2 and occupy most of the study area. Areas with extremely high or low α-values generally occupy a small part of the study area. The areas with extremely low α-values (colored red to dark red) correspond to the regions where the Cu concentrations are enriched. The areas with extremely high α-values (marked by light blue to dark blue) correspond to element-depleted concentrations (Figure 6).

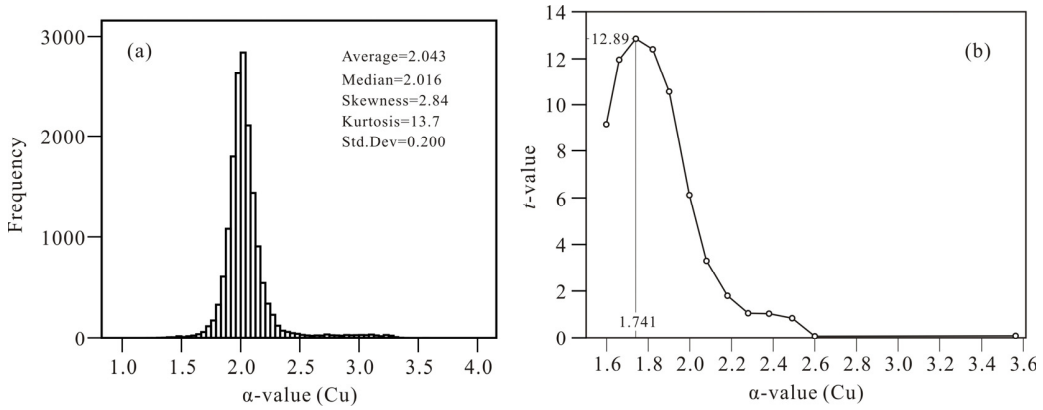

Figure 5. (**a**) Histogram of calculated singularity index of Cu; (**b**) relationship between *t*-value and singularity index value.

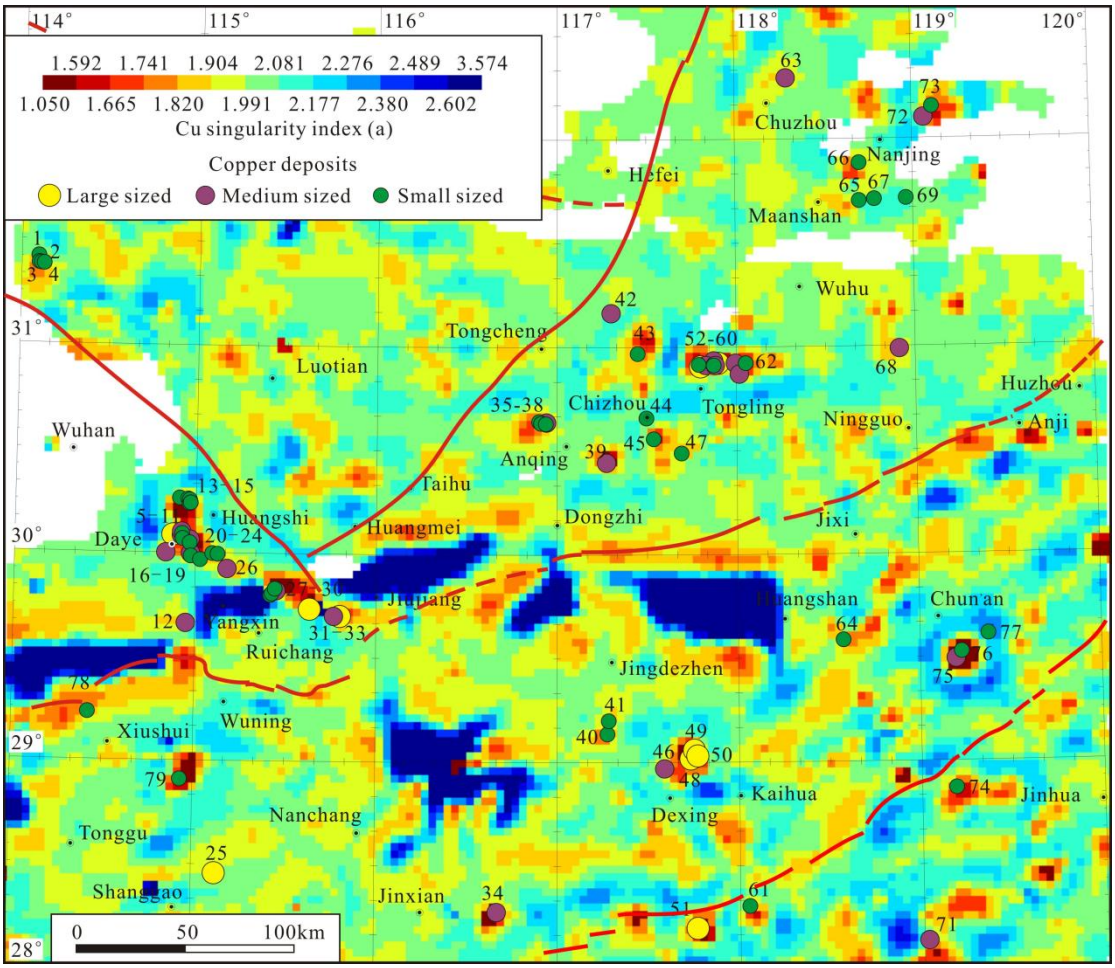

Figure 6. Raster map showing singularity indices of Cu estimated by window-based method.

The relationship between the α-value and the *t*-value is shown in Figure 5b. When the α-value was less than 1.741, the *t*-value increased with the increases in the α-value; when the α-value was greater than 1.741, the α-value decreased with the increases in the α-value. The *t*-value reached a maximum value of 12.89 when the α-value was 1.741. Therefore, we interpret that α = 1.741 is the optimal threshold.

Anomalous patterns created by mineralization processes are often different in terms of spatial and frequency properties. Singularity analysis can effectively reduce the areas of positive anomalies and recognize ore-forming anomalies from complicated geochemical

backgrounds [26]. In Figure 6, the Cu deposits distributed in the geochemical blocks are effectively identified by the singularity indices $\alpha < 1.741$. A total of 9 (90%) of the 10 known large-sized Cu deposits, 13 (59%) of the 22 known medium-sized Cu deposits, and 34 (79%) of the 43 known small-sized Cu deposits are located in the areas with singularity indices $\alpha < 1.741$. The anomalous areas around the Cu deposits are significantly reduced.

5. Discussion

It can be observed from Figure 4 that there is a close spatial correspondence between the Cu deposits and the geochemical blocks in the study area. All five ore districts and one ore field found in the study area are located in the copper geochemical blocks. A total of 8 (80%) of the 10 known large-sized Cu deposits, 15 (68%) of the 22 known medium-sized Cu deposits, and 32 (74%) of the 43 known small-sized Cu deposits are located in the copper geochemical blocks. Therefore, we can conclude that geochemical blocks delineated with low-density geochemical data of one composite value at each grid cell of 10 km by 10 km can effectively track the locations of ore districts or large ore deposits.

Among the six copper geochemical blocks, only Cu1, Cu2, and Cu6 contain ore districts or large ore deposits. So far, only one small-sized Cu deposit has been found in the copper geochemical block Cu4, and two small-sized Cu deposits have been discovered in the copper geochemical block Cu5 (Figure 4). The copper geochemical block Cu4 has a two-layer nested structure, the element concentration of which is relatively low. Thus, we can conclude that not all geochemical blocks contain economic ore deposits, or the potential economic ore deposits in these areas have not been found yet.

Geochemical blocks are usually caused by the effects of rocks with high background values of elements, the enrichment of elements by mineralization, and the secondary dispersion of pre-existing deposits weathering [7]. From the above discussion, we can observe that there are no or few deposits in some large-scale geochemical anomalies, such as in most of the copper geochemical blocks Cu4 and Cu5.

From Table 1, we can observe that among the strata and magmatic rocks in the study area, the Cu concentrations are highest in the Archaean, Proterozoic, Ordovician, Silurian, and mafic magmatic rocks. According to Figures 1 and 4, most of the copper geochemical block Cu4 is occupied by Neoproterozoic strata with high Cu concentrations (Table 1). The rocks distributed in the copper geochemical block Cu5 are mainly Neoproterozoic strata with high Cu concentrations and acid magmatic rocks. Furthermore, most of the rock samples in Figure 2 corresponding to the copper geochemical blocks Cu4 and Cu5 are marked by red dots and show high Cu concentrations (>29.76 μg/g, 80th percentile). Therefore, the copper geochemical blocks Cu4 and Cu5 are mainly caused by the high background value of the rocks and probably not the presence of Cu mineralization.

Table 1. Cu contents (μg/g) in various sedimentary and magmatic rocks in the middle and lower reaches of the Yangtze River and its adjacent areas.

Sample Types	Min.	Max.	Mean	Median	Standard Deviation
Mafic rocks (*N*)	16.45	333.41	104.13	47.98	122.15
Acid rocks (γ)	1.07	156.93	12.89	7.02	20.32
Archaean (Ar)	1.82	34.74	16.18	15.70	10.87
Proterozoic (Pt)	1.20	228.93	24.03	16.94	26.15
Cambrian (Є)	1.33	102.77	16.46	10.09	19.43
Ordovician (O)	1.46	65.12	23.15	17.09	19.78
Silurian (S)	3.79	111.33	28.46	27.74	20.15
Devonian (D)	2.43	46.06	10.44	7.76	10.79
Carboniferous (C)	1.26	37.38	11.46	4.66	12.48
Permian (P)	1.33	126.83	18.91	4.72	29.70
Triassic (T)	1.39	30.73	7.47	5.12	6.82
Jurassic (J)	1.58	67.82	11.23	5.95	12.88
Cretaceous (K)	2.20	41.52	14.82	12.96	9.73
Tertiary (R)	4.30	73.84	15.89	12.27	16.47

The local singularity mapping method can greatly enhance the weak ore-related geochemical anomalies in the study area. The Fenglin (No. 34), Yongping (No. 51), Wuao (No. 71), and Lingshan (No. 74) Cu deposits in Figure 4 are located outside the geochemical blocks or around weak geochemical anomalies. However, in the singularity map (Figure 6), these Cu deposits are spatially coincident with areas with singularity indices a <1.741, colored red to dark red. Thus, the singularity map with high-density geochemical data (4 km × 4 km) can effectively narrow down the anomalous target area and locate the deposits, especially the large deposits.

In Figure 6, the corresponding areas of the copper geochemical blocks Cu4 and Cu5 in Figure 4 are remarkably reduced and decomposed into several smaller anomalies. Only areas with three-layer nested patterns are retained in the singularity maps. These areas are marked by red to dark red with singularity indices a <1.741 and have great potential for prospecting.

The local singularity mapping method can help to complement results based on geochemical blocks with new information it acquires. Patterns obtained from singularity analysis for Cu concentrations can be used to delineate anomalies caused by mineralization and detect mineralization prospects. The combination of the local singularity mapping method and geochemical blocks is useful and applicable for regional prospecting evaluation.

Some areas have low Cu singularity indices, and no mineralization has been identified yet, for example, the bright red region along the eastern boundary of the study area and red regions northeast of 71 (Figure 6). Further mineral exploration in these regions is warranted.

6. Conclusions

(1) All Cu ore districts and a majority of large-scale Cu deposits in the study area are located in the copper geochemical blocks. Geochemical blocks delineated with low-density geochemical data of one composite value at each grid cell of 10 km by 10 km can effectively track the locations of ore districts or large ore deposits.

(2) The singularity mapping method can effectively reduce the areas of anomalies and locate the deposits, especially the large-sized ore deposits, by high-density geochemical data (4 × 4 km).

(3) The combination of geochemical blocks and the local singularity mapping method can delineate the anomalous areas with potential for mineral exploration and can bring out even better results in metallogenic prediction.

Author Contributions: B.L. and X.C.: Conceptualization and Methodology. B.L.: Writing-Original draft preparation. X.C.: Date analysis. X.W.: Data curation. All authors have read and agreed to the published version of the manuscript.

Funding: This research was funded by the Hebei Major Scientific and Technological Achievements Transformation Project (19057411Z) and the National Key R&D Program of Deep-penetrating Geochemistry (2016YFC0600600).

Data Availability Statement: Correspondence and requests for materials should be addressed to X.W.

Acknowledgments: The authors thank Qinping Tan from State Key Laboratory of Ore Deposit Geochemistry, Institute of Geochemistry, Chinese Academy of Sciences, and Haicheng Wang from Institute of Resource and Environmental Engineering, Hebei GEO University, for their help with figures. The authors also acknowledge the reviewers' helpful comments.

Conflicts of Interest: The authors declare no conflict of interest.

References

1. Wang, X.; Xie, X.; Cheng, Z.; Liu, D. Delineation of regional geochemical anomalies penetrating through thick cover in concealed terrains—A case history from the Olympic Dam deposit, Australia. *J. Geochem. Explor.* **1999**, *66*, 85–97. [CrossRef]
2. Wang, X. Exploration geochemistry for giant ore deposits or world-class camps in concealed terrains. *Miner. Depos.* **2000**, *19*, 76–87. (In Chinese with English Abstract)

3. Wang, X. Delineation of geochemical blocks for undiscovered large ore deposits using deep-penetrating methods in alluvial terrains of eastern China. *J. Geochem. Explor.* **2003**, *77*, 15–24. [CrossRef]
4. Cheng, Q. A New Model for Quantifying Anisotropic Scale Invariance and for Decomposition of Mixing Patterns. *J. Int. Assoc. Math. Geol.* **2004**, *36*, 345–360. [CrossRef]
5. Cheng, Q. Multifactal distribution of Eigenvalue and Eigenvectors from 2D multiplicative cascade multifractal fields. *Math. Geol.* **2005**, *37*, 915–927. [CrossRef]
6. Wang, X. China geochemical baselines: Sampling methodology. *J. Geochem. Explor.* **2015**, *148*, 25–39. [CrossRef]
7. Wang, X.; Xu, S.; Chi, Q.; Liu, X. Gold geochemical provinces in China: A micro- and nano-scale formation mechanism. *Acta Geol. Sin.* **2013**, *87*, 1–8. (In Chinese with English Abstract)
8. Wang, X.; Shen, W.; Zhang, B.; Nie, L.; Chi, Q.; Xu, S. Relationship of Geochemical Blocks and Ore Districts: Examples from the Eastern Tianshan Metallogenic Belt, Xinjiang, China. *Earth Sci. Front.* **2007**, *14*, 116–120. [CrossRef]
9. Xie, X.; Liu, D.; Xiang, Y.; Yan, G. Geochemical blocks—Development of concept and methodology. *Geol. China* **2002**, *29*, 225–233. (In Chinese with English Abstract)
10. Xie, X. *Surficial and Superimposed Geochemical Exploration for Giant Ore Deposits*; Clark, A.H., Ed.; Giant Ore Deposits II; Queen's University Press: Kingston, ON, Canada, 1995; pp. 475–485.
11. Liu, D. Development and significance of geochemical blocks. *Geochimica* **2002**, *31*, 539–548. (In Chinese with English Abstract)
12. Cheng, Q. Non-linear mineralization model and information processing methods for prediction of unconventional mineral resources. *J. Earth Sci.* **2003**, *28*, 1–10.
13. Cheng, Q. Non-Linear Theory and Power-Law Models for Information Integration and Mineral Resources Quantitative Assessments. *Math. Geosci.* **2008**, *40*, 503–532. [CrossRef]
14. Zhao, P.; Hu, W.; Li, Z. *Statistical Prediction for Mineral Deposits*, 2nd ed.; Geological Publishing House: Beijing, China, 1994; pp. 113–118. (In Chinese)
15. Zuo, R.; Wang, J. Fractal/multifractal modeling of geochemical data: A review. *J. Geochem. Explor.* **2016**, *164*, 33–41. [CrossRef]
16. Zuo, R.; Carranza, E.J.M.; Wang, J. Spatial analysis and visualization of exploration geochemical data. *Earth-Sci. Rev.* **2016**, *158*, 9–18. [CrossRef]
17. Cheng, Q.; Agterberg, F.; Ballantyne, S. The separation of geochemical anomalies from background by fractal methods. *J. Geochem. Explor.* **1994**, *51*, 109–130. [CrossRef]
18. Deng, J.; Wang, Q.; Wan, L.; Liu, H.; Yang, L.; Zhang, J. A multifractal analysis of mineralization characteristics of the Dayingezhuang disseminated-veinlet gold deposit in the Jiaodong gold province of China. *Ore Geol. Rev.* **2011**, *40*, 54–64. [CrossRef]
19. Wang, Q.; Deng, J.; Zhao, J.; Li, N.; Wan, L. The fractal relationship between orebody tonnage and thickness. *J. Geochem. Explor.* **2012**, *122*, 4–8. [CrossRef]
20. Agterberg, F.; Cheng, Q.; Brown, A.; Good, D. Multifractal modeling of fractures in the Lac du Bonnet Batholith, Manitoba. *Comput. Geosci.* **1996**, *22*, 497–507. [CrossRef]
21. Carranza, E.J.M. Controls on mineral deposit occurrence inferred from analysis of their spatial pattern and spatial association with geological features. *Ore Geol. Rev.* **2009**, *35*, 383–400. [CrossRef]
22. Wan, L.; Wang, Q.; Deng, J.; Gong, Q.; Yang, L.; Liu, H. Identification of Mineral Intensity along Drifts in the Dayingezhuang Deposit, Jiaodong Gold Province, China. *Resour. Geol.* **2010**, *60*, 98–108. [CrossRef]
23. Afzal, P.; Alghalandis, Y.F.; Khakzad, A.; Moarefvand, P.; Omran, N.R. Delineation of mineralization zones in porphyry Cu deposits by fractal concentration–volume modeling. *J. Geochem. Explor.* **2011**, *108*, 220–232. [CrossRef]
24. Li, C.; Ma, T.; Shi, J. Application of a fractal method relating concentrations and distances for separation of geochemical anomalies from background. *J. Geochem. Explor.* **2003**, *77*, 167–175. [CrossRef]
25. Cheng, Q. GeoData Analysis System (GeoDAS) for Mineral Exploration: User's Guide and Exercise Manual. Material for the Training Workshop on GeoDAS Held at York University, Toronto, Canada. 2000, Volume 1–3, p. 204. Available online: http://www.gisworld.org/geodas (accessed on 14 August 2023).
26. Cheng, Q. Mapping singularities with stream sediment geochemical data for prediction of undiscovered mineral deposits in Gejiu, Yunnan Province, China. *Ore Geol. Rev.* **2007**, *32*, 314–324. [CrossRef]
27. Cheng, Q.; Agterberg, F.P. Singularity of mineralization processes and power-law models for mineral resources quantitative assessments. *J. China Univ. Geosci.* **2007**, *18*, 245–247. (In Chinese with English Abstract)
28. Zuo, R.; Cheng, Q. Mapping singularities—A technique to identify potential Cu mineral deposits using sediment geochemical data, an example for Tibet, West China. *Mineral. Mag.* **2008**, *72*, 531–534. [CrossRef]
29. Zuo, R.; Cheng, Q.; Agterberg, F.; Xia, Q. Application of singularity mapping technique to identify local anomalies using stream sediment geochemical data, a case study from Gangdese, Tibet, western China. *J. Geochem. Explor.* **2009**, *101*, 225–235. [CrossRef]
30. Zuo, R.; Xia, Q.; Zhang, D. A comparison study of the C–A and S–A models with singularity analysis to identify geochemical anomalies in covered areas. *Appl. Geochem.* **2013**, *33*, 165–172. [CrossRef]
31. Bai, J.; Porwal, A.; Hart, C.; Ford, A.; Yu, L. Mapping geochemical singularity using multifractal analysis: Application to anomaly definition on stream sediments data from Funin Sheet, Yunnan, China. *J. Geochem. Explor.* **2010**, *104*, 1–11. [CrossRef]

32. Xiao, F.; Chen, J.; Zhang, Z.; Wang, C.; Wu, G.; Agterberg, F.P. Singularity mapping and spatially weighted principal component analysis to identify geochemical anomalies associated with Ag and Pb-Zn polymetallic mineralization in Northwest Zhejiang, China. *J. Geochem. Explor.* **2012**, *122*, 90–100. [CrossRef]
33. Lu, Q.; Yang, Z.; Yan, J.; Xu, W. The metallogenic potential, prospecting idea and primary attempt in depth of the ore belt of the Middle and Lower Reach of the Yangtze River—A case study of Tongling ore district. *Acta Geol. Sin.* **2007**, *81*, 865–881. (In Chinese with English Abstract)
34. Chang, Y.; Liu, X.; Wu, Y. *Metallogenic Belt of the Middle and Lower Yangtze River*; Geological Publishing House: Beijing, China, 1991; pp. 71–76. (In Chinese)
35. Zhai, Y.; Yao, S.; Lin, X. *Regularities of Metallogenesis for Copper (Gold) Deposits in the Middle–Lower Yangtze River Region Area*; Geological Publishing House: Beijing, China, 1992; pp. 1–120. (In Chinese)
36. Mao, J.; Holly, S.; Du, A.; Zhou, T.; Mei, Y.; Li, Y.; Zang, W.; Li, J. Molybdenite Re-Os precise dating for molybdenite from Cu-Au-Mo deposits in the Middle-Lower reaches of Yangtze River belt and its implications for mineralization. *Acta Geol. Sin.* **2004**, *78*, 121–131. (In Chinese with English Abstract)
37. Zhou, T.; Fan, Y.; Yuan, F. Advances on petrogensis and metallogeny study of the mineralization belt of the Middle–Lower Yangtze River region area. *Acta Petrol. Sin.* **2008**, *24*, 1665–1678. (In Chinese with English Abstract)
38. Dong, S.; Ma, L.; Liu, G.; Xue, H.; Shi, W.; Li, J. On Dynamics of metallogenic belt of Middle-Lower reaches of Yangtze River, eastern China. *Acta Geol. Sin.* **2011**, *85*, 612–625. (In Chinese with English Abstract)
39. Xu, S.; Wang, X.; Zhang, B.; Nie, L.; Chi, Q. Geochemical characteristics response of different scales of data: A case study of gold element from 1:200000 regional data of Middle-Lower Reaches of the Yangtze River. *Geophys. Geochem. Explor.* **2012**, *36*, 27–32. (In Chinese with English Abstract)
40. Xu, S.; Wang, W. The significance of different scale copper geochemical anomalies and large ore deposit prediction in the Middle-Lower Yangtze River. *Earth Sci. Front.* **2012**, *19*, 84–92. (In Chinese with English Abstract)
41. Wang, X.; Xu, S.; Chi, Q.; Liu, X.; Wang, W. Accumulation and distribution of metallogenic elements in south China continent. *Geochimica* **2013**, *42*, 229–241. (In Chinese with English Abstract)
42. Liu, B.; Wang, X. Origin of Cu Geochemical Deomains in the Middle-Lower Yangtze River Region and Its Constraints on the Formation of Cu Deposit Districts. *Bull. Mineral. Petrol. Geochem.* **2018**, *37*, 271–282. (In Chinese with English Abstract)
43. Mao, J.; Shao, Y.; Xie, G.; Zhang, J.; Chen, Y. Mineral deposit model for porphyry-skarn polymetallic copper deposits in Tongling ore dense district of Middle-Lower Yangtze Valley Metallogenic belt. *Miner. Depos.* **2009**, *28*, 109–119. (In Chinese with English Abstract)
44. Gao, L.; Ding, X.; Pang, W.; Zhang, C. New geological time scale of Late Precambrian in China and geochronology. *Geol. China* **2010**, *37*, 1014–1020. (In Chinese with English Abstract)
45. Liu, B.; Wang, X.; Hou, Q. Temporal distribution of copper geochemical blocks in the Middle–Lower Yangtze River region: Evidence from detrital zircon LA-ICP-MS U-Pb dating. *Acta Geosci. Sin.* **2020**, *41*, 835–850. (In Chinese with English Abstract)
46. Zhou, T.; Fan, Y.; Yuan, F.; Zhang, L.; Ma, L.; Qian, B.; Xie, J. Petrogensis and metallogeny study of the volcanic basins in the Middle and Lower Yangtze metallogenic belt. *Acta Geol. Sin.* **2011**, *85*, 712–730. (In Chinese with English Abstract)
47. Li, H.; Ling, M.-X.; Li, C.-Y.; Zhang, H.; Ding, X.; Yang, X.-Y.; Fan, W.-M.; Li, Y.-L.; Sun, W.-D. A-type granite belts of two chemical subgroups in central eastern China: Indication of ridge subduction. *Lithos* **2012**, *150*, 26–36. [CrossRef]
48. Li, J.; Zhao, X.; Zhou, M.; Vasconcelos, P.; Ma, C.; Deng, X.; Sérgio de Souza, Z.; Zhao, Y.; Wu, G. Origin of the Tongshankou porphyry-skarn Cu-Mo deposit, eastern Yangtze craton, Eastern China: Geochronological, geochemical, and Sr-Nd-Hf isotopic constraints. *Miner. Depos.* **2008**, *43*, 315–336. [CrossRef]
49. Zhou, T.; Fan, Y.; Yuan, F.; Zhong, G. Progress of geological study in the Middle-Lower Yangtze River Vallley metallogenic belt. *Acta Petrol. Sin.* **2012**, *28*, 3051–3066, (In Chinese with English Abstract).
50. Wang, Y.; Zhang, Q.; Wang, Y. Geochemical characteristics of volcanic rocks from Ningwu area, and its significance. *Acta Petrol. Sin.* **2001**, *17*, 565–575. (In Chinese with English Abstract)
51. Xie, X.; Ma, X.; Ren, T. Geochemical mapping in China. *J. Geochem. Explor.* **1997**, *60*, 99–113.
52. Doe, B.R. Source rock and the genesis of metallic mineral deposits. *Glob. Tecton. Metallog.* **1991**, *4*, 13–19. [CrossRef]
53. Xie, X. *Geochemical Prediction Method for Giant Ore Deposits*; Xie, X., Shao, Y., Wang, X., Eds.; Exploration Geochemistry Into 21st Century; Geological Publishing House: Beijing, China, 1999; pp. 61–69. (In Chinese)
54. Gao, Y.; Chen, J.; Zhang, Y.; Wang, W. Further research on geochemical mapping. *Comput. Tech. Geophys. Geochem. Explor.* **2015**, *37*, 538–546. (In Chinese with English Abstract)
55. Gao, Y.; Li, J.; Chen, J.; Zhang, Y.; Wang, W. The visualization of iteration processing of geochemical exploration data and an analysis of the result. *Geophys. Geochem. Explor.* **2016**, *40*, 1021–1025. (In Chinese with English Abstract)
56. Gao, Y.; Liu, Q.; Wang, W.; Wang, W. The discussing of normal distribution and long value in geochemical exploration. *Comput. Tech. Geophys. Geochem. Explor.* **2017**, *39*, 404–410. (In Chinese with English Abstract)
57. Agterberg, F.P. Multifractals and geostatistics. *J. Geochem. Explor.* **2012**, *122*, 113–122. [CrossRef]

Disclaimer/Publisher's Note: The statements, opinions and data contained in all publications are solely those of the individual author(s) and contributor(s) and not of MDPI and/or the editor(s). MDPI and/or the editor(s) disclaim responsibility for any injury to people or property resulting from any ideas, methods, instructions or products referred to in the content.